



# Production, composition, and mode of action of the painful defensive venom produced by a limacodid caterpillar, *Doratifera vulnerans*

Andrew A. Walker<sup>a,1</sup>, Samuel D. Robinson<sup>a</sup>, Jean-Paul V. Paluzzi<sup>b</sup>, David J. Merritt<sup>c</sup>, Samantha A. Nixon<sup>a,d</sup>, Christina I. Schroeder<sup>a,2</sup>, Jiayi Jin<sup>a</sup>, Mohaddeseh Hedayati Goudarzi<sup>a</sup>, Andrew C. Kotze<sup>d</sup>, Zoltan Dekan<sup>a</sup>, Andy Sombke<sup>e</sup>, Paul F. Alewood<sup>a</sup>, Bryan G. Fry<sup>c</sup>, Marc E. Epstein<sup>f</sup>, Irina Vetter<sup>a,g</sup>, and Glenn F. King<sup>a,1</sup>

<sup>a</sup>Institute for Molecular Bioscience, The University of Queensland, St Lucia, QLD, 4072, Australia; <sup>b</sup>Department of Biology, York University, Toronto, ON M3J 1P3, Canada; <sup>c</sup>School of Biological Sciences, The University of Queensland, St. Lucia, QLD, 4072, Australia; <sup>d</sup>CSIRO Agriculture and Food, Queensland Bioscience Precinct, St Lucia, QLD, 4072, Australia; <sup>e</sup>Department of Evolutionary Biology, Integrative Zoology, University of Vienna, 1090 Vienna, Austria; <sup>f</sup>Plant Pest Diagnostics Branch, California Department of Food and Agriculture, Sacramento, CA 95832-1448; and <sup>g</sup>School of Pharmacy, The University of Queensland, Woollongabba, QLD, 4102, Australia

Edited by John G. Hildebrand, University of Arizona, Tucson, AZ, and approved March 1, 2021 (received for review November 17, 2020)

**Venoms have evolved independently several times in Lepidoptera. Limacodidae is a family with worldwide distribution, many of which are venomous in the larval stage, but the composition and mode of action of their venom is unknown. Here, we use imaging technologies, transcriptomics, proteomics, and functional assays to provide a holistic picture of the venom system of a limacodid caterpillar, *Doratifera vulnerans*. Contrary to dogma that defensive venoms are simple in composition, *D. vulnerans* produces a complex venom containing 151 proteinaceous toxins spanning 59 families, most of which are peptides <10 kDa. Three of the most abundant families of venom peptides (vulnericins) are 1) analogs of the adipokinetic hormone/corazonin-related neuropeptide, some of which are picomolar agonists of the endogenous insect receptor; 2) linear cationic peptides derived from cecropin, an insect innate immune peptide that kills bacteria and parasites by disrupting cell membranes; and 3) disulfide-rich knottins similar to those that dominate spider venoms. Using venom fractionation and a suite of synthetic venom peptides, we demonstrate that the cecropin-like peptides are responsible for the dominant pain effect observed in mammalian *in vitro* and *in vivo* nociception assays and therefore are likely to cause pain after natural envenomations by *D. vulnerans*. Our data reveal convergent molecular evolution between limacodids, hymenopterans, and arachnids and demonstrate that lepidopteran venoms are an untapped source of novel bioactive peptides.**

venom peptide | Limacodidae | Lepidoptera | cecropin | toxin

**W**hile adult lepidopterans are specialized for dispersal and mating, their larvae are specialized for plant-feeding and growth. A potential disadvantage of this life history is that caterpillars are vulnerable to predators, lacking physical defenses such as teeth or claws or the ability to flee rapidly. Thus, caterpillars have evolved a multitude of biological defenses including irritative hairs, toxins that render them poisonous to eat, spots that mimic snake eyes, or spines that inject liquid venoms. Unsurprisingly, given that many caterpillar predators are vertebrates, lepidopteran venoms can have striking effects on humans. For example, venom of the Brazilian taturana (Saturniidae: *Lonomia* sp.) has been studied extensively due to its ability to induce coagulopathy and hemorrhagic syndrome in humans, which sometimes results in fatalities (1).

Recent phylogenomic studies support multiple independent origins of venom in Lepidoptera, a hyperdiverse insect order that comprises >150,000 described species in 34 superfamilies (2, 3). For example, many members of the superfamily Zygaenoidea, especially those in the families Limacodidae and Megalopygidae, inject potent, pain-inducing liquid venoms that deter potential predators. Yet, in contrast to the numerous studies on the venom of *Lonomia* species, almost nothing is known about the venom

systems of zygaenoid caterpillars. The vast phylogenetic distance between Zygaenoidea and *Lonomia* sp. (superfamily Bombycoidea), as well as the very different symptoms resulting from envenomation by these caterpillars, indicates that these two groups evolved venom use independently (*SI Appendix, Fig. S1*) (2, 3). For this reason, a detailed analysis of a zygaenoid venom system represents an ideal way to obtain new and independent data on the detailed evolutionary processes that underlie the evolution of venom use. For example, current theories of venom evolution focus on the convergent recruitment of endogenous polypeptides with intrinsically toxin-like properties (4) and toxin divergence driven by gene duplication and neofunctionalization (5), but the relative importance of these processes and their relationship to the ecological use of venom is currently debated (6, 7). Moreover, the discovery of new types of peptide and protein toxins may

## Significance

**Venoms of limacodid caterpillars evolved independently to those of previously studied animals, and analysis of their venom therefore provides an opportunity to examine patterns of molecular convergence and divergence underlying the evolution of venom use. We report remarkable convergence in the recruitment of venom peptides between limacodids and other venomous taxa. Like scorpions and spiders, limacodids have weaponized immune system peptides to deter potential predators, although these cecropin-derived venom peptides are more similar in structure and mode of action to the venom peptides of hymenopteran insects. This study reveals a venom system with a unique combination of features not previously reported in other venomous animals and provides insights into the functional basis of venoms of the Limacodidae.**

Author contributions: A.A.W., S.D.R., J.-P.V.P., D.J.M., S.A.N., C.I.S., Z.D., A.S., M.E.E., I.V., and G.F.K. designed research; A.A.W., S.D.R., J.-P.V.P., D.J.M., S.A.N., C.I.S., J.J., M.H.G., Z.D., A.S., and I.V. performed research; A.A.W., S.D.R., J.-P.V.P., D.J.M., C.I.S., A.C.K., A.S., P.F.A., B.G.F., I.V., and G.F.K. contributed new reagents/analytic tools; A.A.W., S.D.R., J.-P.V.P., D.J.M., S.A.N., C.I.S., A.S., I.V., and G.F.K. analyzed data; and A.A.W., S.D.R., J.-P.V.P., D.J.M., S.A.N., C.I.S., J.J., M.H.G., A.C.K., Z.D., A.S., P.F.A., B.G.F., M.E.E., I.V., and G.F.K. wrote the paper.

The authors declare no competing interest.

This article is a PNAS Direct Submission.

Published under the PNAS license.

<sup>1</sup>To whom correspondence may be addressed. Email: a.walker@imb.uq.edu.au or glenn.king@imb.uq.edu.au.

<sup>2</sup>Present address: Center for Cancer Research, National Cancer Institute, National Institutes of Health, Frederick, MD 21702.

This article contains supporting information online at <https://www.pnas.org/lookup/suppl/doi:10.1073/pnas.2023815118/-DCSupplemental>.

Published April 23, 2021.

yield molecules that can be utilized in biotechnology, agriculture, and medicine (8).

The Limacodidae comprise ~1,650 described species, of which more than half are venomous (9, 10). Envenomations by limacodids typically induce intense pain, itch, and erythema, and sometimes numbness, weakness, nausea, and dizziness (11). Venom use may have evolved within Limacodidae (10) or in a shared ancestor of Limacodidae and Megalopygidae with subsequent losses in related taxa (12). Limacodid venom has been shown to protect caterpillars against invertebrate predators, and this protection is stronger for predators previously exposed to the venom, indicating that envenomation induces learned avoidance in some predators (13). Some predators nevertheless prey upon venomous limacodids after chewing off the venom spines (wasps), piercing the underside of the caterpillar from the opposite side of the leaf (assassin bugs), or after rubbing the venom spines on the ground to discharge them (macaques) (13, 14). The palatable nature of limacodids when their venomous spines can be circumvented, which is in contrast to some other zygaenoid caterpillars that are poisonous when eaten (15), is likely to confer adaptive fitness to the trait of venom use.

The most detailed information available on the composition and function of limacodid venom comes from studies on the Asian limacodid *Parasa consocia* Walker, 1865 (16). Injection of venom into the tail vein of mice caused nocifensive behavior (licking the site of injury, crouching, and shivering) or limb paralysis when venom was injected subcutaneously (17). Both high- (>15 kDa) and low- (<15 kDa)-molecular-mass fractions induced contraction of guinea pig ileum, increased vascular permeability, and caused pain when injected into human volunteers. More rapid onset and resolution of pain responses was reported for the low-molecular-mass fraction. The active components of the low-molecular-mass fraction were reported to be histamine and a “peptide of several thousand [Daltons]” that was suggested to have kinin-like properties (17).

Here, we report a holistic description of the venom system of a larval limacodid, the painted cup moth caterpillar *Doratifera vulnerans* (Lewin, 1805) (18). This species, whose binomial name etymologically means “bearer of painful gifts,” is a common culprit of caterpillar envenomations in Australia. Microscopy and imaging technologies revealed the morphology and physiology of the limacodid venom-producing apparatus. Venom proteomics combined with a transcriptome of tissue including the venom-secreting cells allowed us to resolve a venom proteome of 151 polypeptides, most of which are peptides <10 kDa. We identify several algogenic peptides that directly activate mammalian pain-sensing neurons by permeabilizing cell membranes. These findings reveal numerous insights into limacodid biology and venom evolution.

## Results

**Each Spine Is an Independent Munition for Production, Storage, and Injection of Venom.** Larvae of *D. vulnerans* are endowed with venomous spines. Like all members of the genus *Doratifera*, the groups of large venom spines (dorsal scoli) are retracted at rest (Fig. 1A) and everted when the animal is disturbed (Fig. 1B and Movie S1), a behavior that is possibly an adaptation to prevent premature discharge of venom from the spines. The adult moth (Fig. 1C) does not have spines. In mid- and late-instar *D. vulnerans*, the eight venom scoli are arranged symmetrically on segments T3, A1, A7, and A8 (Fig. 1D and E). During observation of living and dissected caterpillars we observed that an entirely new set of eight scoli, each bearing 50 to 100 spines, is grown for each instar stage and sloughed and discarded together with any venom they contain each time the caterpillar molts. For a short time after apolysis but before ecdysis, the caterpillar possesses two complete sets of eight scoli: one on the outer old cuticle to be sloughed, and one on the new inner cuticle of the next instar.

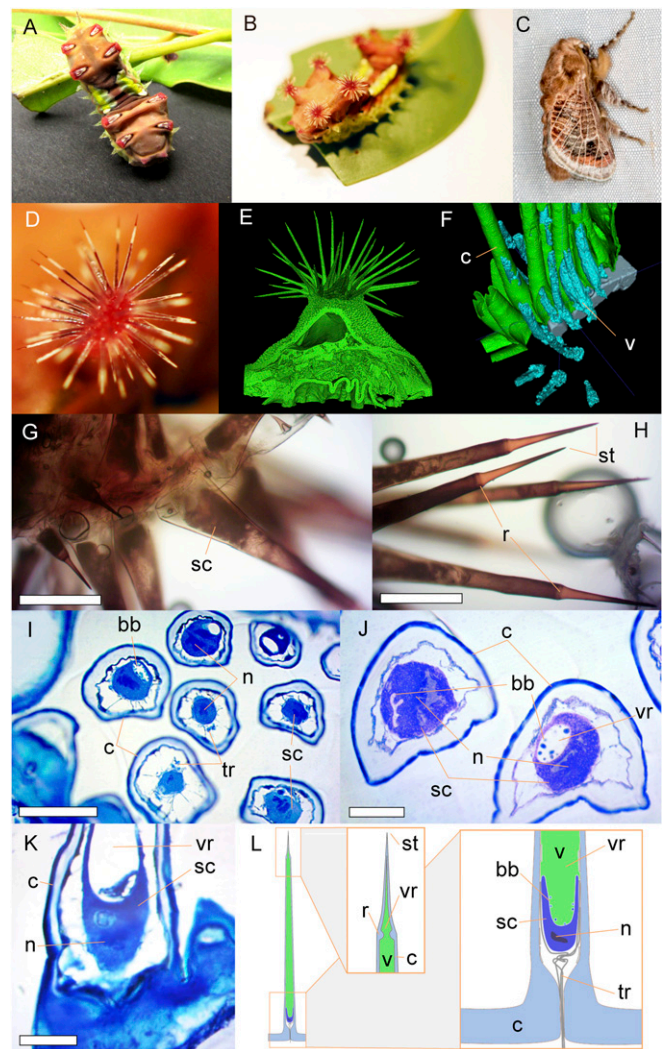


**Fig. 1.** Morphology and venom apparatus of the limacodid caterpillar *D. vulnerans*. (A) Final instar caterpillar in resting posture with spines folded against body, length ~25 mm. Image credit: Mount Gravatt Environment Group. (B) Final instar caterpillar in defense posture with eight scoli of everted venom spines. (C) Nonvenomous adult moth, length ~18 mm. Image credit: Flickr/lan MacMillan. (D) Left anterior-most venom scolus, ~6 mm across. (E and F)  $\mu$ -CT reconstructions of fixed specimens. (E) Venom scolus and surrounding tissue. (F) Venom spines showing venom (v, blue) and cuticle (c, green). (G and H) Light micrographs of shed exuviae. (Scale bar, 100  $\mu$ m.) (G) Base of venom spines with secretory cell (sc) visible. (H) Distal ends of spines with rings (r) and spine tips (st). (I–K) Light micrographs of resin-embedded specimens. (I) Slice through the base of spines. Secretory cells (sc) with associated trachea (tr) encased in cuticle, with nuclei (n) and brush borders (bb) visible. (Scale bar, 100  $\mu$ m.) (J) Higher magnification micrograph through base of spines with venom reservoir (vr) visible. (Scale bar, 40  $\mu$ m.) (K) Slice through base approximately longitudinal to spine, showing cup-shaped secretory cell. (Scale bar, 40  $\mu$ m.) (L) Schematic of an individual spine and its functional anatomy for the production, storage, and delivery of venom (green).

Light microscopy of sections through the spines revealed that these cuticular structures contain a central reservoir extending throughout the spine in which venom is visible as an aggregated, granular material in formalin-fixed samples by microcomputed tomography ( $\mu$ -CT) (Fig. 1F). A single large (~50  $\mu$ m diameter) nucleated cell is present at the base of each spine (Fig. 1G) whereas at the distal end, the spine takes on a distinctive needle-like shape (Fig. 1H). The apical surface of the cell inside the base of the spine forms the bottom of the spine lumen. At the interface



between this cell and the spine lumen, the plasma membrane forms a brush border consistent with an active secretory surface (Fig. 1 I–K). A characteristic arrangement of small-diameter trachea extends from the hemolymph and clusters around the secretory cell body, presumably to supply this energetically demanding but cuticle-bound cell with oxygen (Fig. 1L). Our data indicate that each spine represents an independent unit capable of producing, storing, and injecting venom and suggest that messenger RNA isolated from scoli tissue should contain toxin-encoding transcripts.

**Venom Comprises a Diverse Array of Peptide Toxins.** Previous studies of caterpillar venom relied on crushed extracts of spines or spicules, but such extracts invariably contain cellular and cuticular material, which complicates identifying venom components using transcriptomic and proteomic workflows (19). To overcome this obstacle, we obtained venom by gently pressing parafilm supported on a wire loop to the tips of venom spines. This simple procedure resulted in hundreds of tiny droplets of venom per caterpillar that we recovered with 5  $\mu$ L ultrapure water and lyophilized.

To investigate the polypeptide composition of *D. vulnerans* venom, we combined proteomic examination of venom with transcriptomics of the venom scoli (SI Appendix, Supplementary Methods). We extracted 34.4  $\mu$ g of total RNA from the venom scoli of a newly molted final instar caterpillar, from which poly-A<sup>+</sup> RNA was isolated and sequenced using the Illumina platform. This yielded 31,377,889 paired-end 150 bp reads, which were assembled using Trinity (20) and CLC Genomics Workbench software packages, producing 1,312,527 total contigs. According to the Benchmarking Universal Single-Copy Orthologs algorithm (21), this transcriptome contained 95.2% of arthropod core genes. After removal of redundant contigs using CD-HIT-EST (22), 1,324,013 open reading frames (ORFs) of >25 amino acids in length were extracted and translated in silico to form a search database. To identify venom toxins from this sequence database, we obtained multiple liquid chromatography–tandem mass spectrometry (LC-MS/MS) datasets from venom that was either untreated, reduced and alkylated, or reduced, alkylated, and trypsinized (SI Appendix, Supplementary Methods). The identified sequences were annotated using SignalP (23), HMMER (24), and BLAST (25) algorithms.

*D. vulnerans* venom contains a rich diversity of polypeptides. By searching spectra from the reduced, alkylated, and trypsinized venom samples, we identified 138 polypeptide precursors. Additionally, 72 intact mature peptides were detected with high confidence from the reduced and alkylated (but not trypsinized) sample. Overall, we report a total of 151 polypeptide sequences that contribute to the venom proteome. For the 72 peptides detected in the nontrypsinized venom samples, we were able to assign the position of N and C termini and posttranslational modifications (PTMs). We annotated polypeptides according to sequence homology, grouped them into 59 different families (Table 1), and named them according to rational nomenclature guidelines (26). For example, for the peptide U-LCTX<sub>3</sub>-Dv32a, the prefix “U” indicates unknown bioactivity, “LCTX” is an abbreviation of limacoditoxin, the subscript “3” indicates a putative family of homologous peptides, the number “32” is a unique peptide identifier, and the letter “a” is used to denote minor sequence variants. Since our transcriptome is derived from both venom-secreting cells and also surrounding tissues, we estimated toxin expression levels as transcripts per million toxin-encoding transcripts (Dataset S1, column AO). Additional information on toxin abundance is present in the signal attributed to each toxin in a matrix-assisted laser desorption/ionization time-of-flight (MALDI-TOF) reflectron-positive venom mass spectrum (Dataset S1, column AI) and the reverse-phase (RP) HPLC chromatogram shown in Fig. 2F. These data constitute a

detailed venom proteome for *D. vulnerans* and provide insights into the venoms of limacodid caterpillars.

*D. vulnerans* venom is dominated by peptide toxins (Fig. 2). When analyzed using sodium dodecyl sulfate polyacrylamide gel electrophoresis, venom from *D. vulnerans* and the congener *Doratifera casta* show intense bands <10 kDa (Fig. 2A). *D. vulnerans* venom displayed no other major bands, while *D. casta* venom yielded several minor bands of 10 to 15 kDa and 21 kDa. Of the 151 polypeptides detected in *D. vulnerans* venom by proteomics, 110 (73%) were peptides (classified here as those with dominant mature proteoforms <100 amino acids in length). A total of 91.4% of toxin transcripts encoded peptides, whereas only 8.6% encoded larger toxins (Fig. 2B). Many toxins (42 of 151, or 28%, more than other bins considered) were of 31 to 40 amino acid residues in length (Fig. 2C, Upper). Polypeptides with an even number of cysteine residues were much more numerous than those with odd numbers (143 and 8 polypeptides, respectively), with the majority of peptides having either zero or six cysteines (62 and 55 polypeptides, respectively) (Fig. 2C, Lower). Thus, the majority of peptide toxins in *D. vulnerans* venom are either devoid of cysteine residues or are “knottins,” disulfide-rich venom peptides that contain intrachain disulfide bridges (Dataset S1).

**Knottins, Neurohormones, and Cecropins: Major Limacodid Venom Peptides.** Of the 59 polypeptide families detected in venom, 3 were particularly prominent, with multiple peptide representatives and high abundance in venom. For example, U-LCTX<sub>1</sub>-Dv4 (ZITFSKDWRP-NH<sub>2</sub>) was an extremely abundant peptide in *D. vulnerans* venom (Fig. 2D–F). Almost one-quarter (23.8%) of all toxin-encoding transcripts encoded Dv4, which also accounted for the highest peaks in the MALDI-TOF reflectron-positive mass spectrum (Fig. 2D) and reversed-phase high-performance liquid chromatography (RP-HPLC) chromatogram (Fig. 2F). Dv4 is a member of limacoditoxin Family 1, which contains eight peptides each having 9 to 10 residues, beginning with a pyroglutamate residue and ending (in all but one case) in an  $\alpha$ -amidated residue at the C terminus. These peptides are similar to adipokinetic hormone/corazonin-related peptide (ACP), an insect neuro-peptide that signals through a G protein-coupled receptor (GPCR). ACP and its receptor (ACPR) are homologous to the mammalian gonadotropin-releasing-hormone signaling system, and they are widespread among arthropods (27). One *D. vulnerans* peptide, U-LCTX<sub>1</sub>-Dv1 (ZVTFSRDWGP-NH<sub>2</sub>), differs by only one residue from the natural hormone present in the red flour beetle *Tribolium castaneum* (ZVTFSRDWNP-NH<sub>2</sub>), while other members of venom peptide Family 1 are more divergent. These data suggest that ACP, which shows strong sequence conservation across broad phylogenetic ranges (e.g., crustaceans and insects; Fig. 3A, Left) has been recruited as a venom peptide in Limacodidae and then undergone gene duplication and accelerated sequence divergence, similar to that reported for some venom toxins from other animal groups (5, 28). This hypothesis is supported by the observation that the precursors of Family 1 venom peptides differ in structure from the evolutionarily conserved architecture of nonvenom ACP precursors, which feature a long C-terminal pro-peptide that is removed enzymatically (Fig. 3A, Right).

Family 2 consists of linear peptides comprising 14 to 85 residues, including many (15 to 24%) cationic residues. A typical example and the most abundant member of this family is U-LCTX<sub>2</sub>-Dv11 (KRGFGKLLRKVFKVGRVAGSAAEISGSSGGEE). Some Family 2 peptide precursors are clearly homologous to a family of peptides that includes the cecropins, hinnavins, and moricins, which are peptides produced by nonvenomous Lepidoptera that function in innate immunity and have cytolytic, antimicrobial, antifungal, and antiparasitic activities (Fig. 3B and Dataset S1) (29). These peptides also display structural similarities to the aculeotoxins, which are the major components of venoms produced by hymenopteran insects (30).

**Table 1. Polypeptide families in *D. vulnerans* venom**

| Family No. | members | No. of residues | No. of Cys residues | Generalized structure   | Homology                            |
|------------|---------|-----------------|---------------------|---|-------------------------------------|
| 1          | 8       | 9–10            | 0                   | ZX <sub>8-9</sub> #   | ACP                                 |
| 2          | 11      | 14–85           | 0                   | X <sub>14-85</sub> , cationic   | Cecropin                            |
| 3          | 41      | 28–53           | 6                   | X <sub>0-7</sub> CX <sub>6-7</sub> CX <sub>4-14</sub> CCX <sub>3-5</sub> CX <sub>4-9</sub> CX <sub>1-17</sub>   | ICK                                 |
| 4          | 6       | 34              | 0                   | X <sub>34</sub> , cationic  | None                                |
| 5          | 5       | 24–31           | 2                   | X <sub>4-6</sub> CX <sub>8-9</sub> CX <sub>8-17</sub> #, cationic   | None                                |
| 6          | 1       | 27              | 4                   | X <sub>4</sub> CX <sub>6</sub> CX <sub>5</sub> CCX <sub>8</sub>   | None                                |
| 7          | 6       | 17–45           | 0                   | X <sub>17-45</sub>  | None                                |
| 8          | 1       | 31              | 0                   | X <sub>31</sub> #   | Calcitonin-like DH <sub>31</sub>    |
| 9          | 2       | 115             | 10                  | XCCX <sub>16</sub> CX <sub>21</sub> CX <sub>11</sub> CX <sub>4</sub> CX <sub>4</sub> CX <sub>3</sub> CX <sub>40</sub>   | Diedel                              |
| 10         | 2       | 77              | 6                   | X <sub>5</sub> CX <sub>11</sub> CX <sub>10</sub> CX <sub>6</sub> CX <sub>5</sub> CX <sub>10</sub> CX <sub>24</sub>  | LDL receptor A domain               |
| 11         | 4       | 182–190         | 0–3                 | Most are linear   | Calcectin                           |
| 12         | 1       | 12              | 0                   | X <sub>12</sub> #   | None                                |
| 13         | 1       | 14              | 0                   | X <sub>14</sub> #   | None                                |
| 14         | 3       | 16–30           | 0–2                 | Most are linear   | None                                |
| 15         | 2       | 40              | 6                   | X <sub>2</sub> CX <sub>6</sub> CX <sub>5</sub> CX <sub>11</sub> CX <sub>3</sub> CX <sub>2</sub> CX <sub>5</sub>   | None                                |
| 16         | 2       | 53–55           | 6                   | X <sub>3-5</sub> CX <sub>7-8</sub> CX <sub>10</sub> CX <sub>21-24</sub> CX <sub>3-5</sub>   | Kazal domain                        |
| 17         | 2       | 85              | 6                   | X <sub>12</sub> CX <sub>15</sub> CX <sub>2</sub> CX <sub>12</sub> CX <sub>3</sub> CX <sub>8</sub> CX <sub>27</sub>  | ITP/CHH                             |
| 18         | 1       | 85              | 12                  | X <sub>3</sub> CX <sub>4</sub> CX <sub>8</sub> CX <sub>13</sub> CX <sub>2</sub> CX <sub>9</sub> CX <sub>14</sub> CX <sub>5</sub> CX <sub>4</sub> CX <sub>6</sub> #  | Fungal protease inhibitor           |
| 19         | 5       | 103–110         | 0                   | X <sub>103-110</sub>  | Reduvitoxin family 3, Asilitoxin-11 |
| 20         | 3       | 127             | 10                  | X <sub>18</sub> CX <sub>8</sub> CX <sub>6</sub> CX <sub>18</sub> CX <sub>2</sub> CX <sub>12</sub> CX <sub>4</sub> CX <sub>31</sub> CX <sub>3</sub> CX <sub>5</sub> CX <sub>9</sub>                                      | Odorant binding protein             |
| 21         | 2       | 132–139         | 4                   | X <sub>20</sub> CX <sub>32</sub> CX <sub>38</sub> CX <sub>1</sub> 8CX <sub>21-28</sub>  | Odorant binding protein             |
| 22         | 1       | 12              | 0                   | X <sub>12</sub>   | None                                |
| 23         | 2       | 27–29           | 0                   | X <sub>27-29</sub>  | None                                |
| 24         | 1       | 11              | 0                   | X <sub>11</sub>   | None                                |
| 25         | 1       | 139             | 9                   | X <sub>30</sub> CX <sub>5</sub> CX <sub>14</sub> CX <sub>4</sub> CX <sub>16</sub> CX <sub>9</sub> CX <sub>15</sub> CCX <sub>4</sub> CX <sub>33</sub>  | VWF                                 |
| 26         | 1       | 148             | 2                   | X <sub>9</sub> CX <sub>76</sub> CX <sub>61</sub>  | Reeler domain                       |
| 27         | 1       | 152             | 4                   | X <sub>38</sub> CX <sub>39</sub> CX <sub>4</sub> CX <sub>54</sub>   | None                                |
| 28         | 2       | 156             | 6                   | X <sub>24</sub> CX <sub>13</sub> CX <sub>39</sub> CX <sub>67</sub> CX <sub>5</sub>  | None                                |
| 30         | 1       | 165             | 12                  | ZX <sub>12</sub> CX <sub>12</sub> CCX <sub>13</sub> CX <sub>19</sub> CX <sub>4</sub> CX <sub>43</sub> CX <sub>11</sub> CX <sub>7</sub> CX <sub>8</sub> CX <sub>9</sub> CX <sub>6</sub>                                  | Odorant binding protein             |
| 31         | 1       | 170             | 0                   | X <sub>170</sub>  | Apolipoprotein-III                  |
| 32         | 1       | 211             | 1                   | X <sub>83</sub> CX <sub>127</sub>   | Hsp20                               |
| 34         | 1       | 192             | 1                   | X <sub>146</sub> CX <sub>45</sub>   | Distal rod protein                  |
| 35         | 1       | 226             | 0                   | X <sub>226</sub>  | None                                |
| 36         | 1       | 216             | 12                  | ZX <sub>18</sub> CX <sub>21</sub> CX <sub>30</sub> CX <sub>8</sub> CX <sub>10</sub> CX <sub>23</sub> CX <sub>17</sub> CX <sub>10</sub> CX <sub>22</sub> CX <sub>8</sub> CX <sub>7</sub> X <sub>21</sub> CX <sub>8</sub> | None                                |
| 37         | 1       | 217             | 4                   | X <sub>6</sub> CX <sub>6</sub> CX <sub>53</sub> CX <sub>17</sub> CX <sub>131</sub>  | Odorant binding protein             |
| 38         | 1       | 224             | 2                   | X <sub>106</sub> CX <sub>21</sub> CX <sub>95</sub>  | Glutamyl cyclase                    |
| 39         | 1       | 260             | 6                   | X <sub>4</sub> CX <sub>66</sub> CX <sub>14</sub> CX <sub>119</sub> CX <sub>25</sub> CX <sub>26</sub> C  | None                                |
| 40         | 1       | 315             | 3                   | X <sub>110</sub> CX <sub>118</sub> CX <sub>70</sub> CX <sub>14</sub> CX <sub>25</sub>   | None                                |
| 41         | 1       | 320             | 8                   | ZX <sub>21</sub> CX <sub>32</sub> CX <sub>11</sub> CX <sub>17</sub> CX <sub>91</sub> CX <sub>70</sub> CX <sub>20</sub> CX <sub>18</sub> CX <sub>31</sub>  | PAM                                 |
| 42         | 1       | 112             | 2                   | X <sub>8</sub> CX <sub>331</sub> C  | Phosphodiesterase                   |
| 43         | 1       | 369             | 5                   | X <sub>144</sub> CX <sub>134</sub> CX <sub>51</sub> CX <sub>5</sub> CX <sub>22</sub> CX <sub>8</sub>  | Acid phosphatase                    |
| 44         | 1       | 430             | 4                   | X <sub>8</sub> CX <sub>26</sub> CX <sub>283</sub> CX <sub>94</sub> CX <sub>15</sub>   | Chitinase                           |
| 45         | 1       | 476             | 5                   | ZX <sub>65</sub> CX <sub>15</sub> CX <sub>107</sub> CX <sub>46</sub> CX <sub>10</sub> CX <sub>227</sub>   | Carboxylesterase                    |
| 46         | 1       | 606             | 8                   | ZX <sub>116</sub> CX <sub>7</sub> CX <sub>194</sub> CX <sub>17</sub> CX <sub>112</sub> CX <sub>54</sub> CX <sub>17</sub> CX <sub>75</sub> CX <sub>5</sub>   | ACE                                 |
| 47         | 1       | 10              | 0                   | X <sub>10</sub> #   | None                                |
| 48         | 1       | 23              | 0                   | X <sub>23</sub>   | None                                |
| 49         | 1       | 11              | 0                   | X <sub>11</sub>   | None                                |
| 50         | 1       | 12              | 0                   | X <sub>12</sub>   | None                                |
| 51         | 1       | 17              | 0                   | X <sub>17</sub>   | None                                |
| 52         | 1       | 12              | 0                   | X <sub>12</sub> #   | None                                |
| 53         | 2       | 28              | 0                   | X <sub>28</sub>   | None                                |
| 55         | 1       | 14              | 0                   | Multiple products (see <i>SI Appendix, Fig. S4</i> )  | None                                |
| 56         | 1       | 30              | 0                   | X <sub>30</sub>   | None                                |
| 57         | 1       | 21              | 0                   | X <sub>21</sub>   | None                                |
| 58         | 1       | 28              | 3                   | X <sub>11</sub> CX <sub>4</sub> CX <sub>10</sub> C  | None                                |
| 59         | 1       | 13              | 0                   | X <sub>13</sub>   | None                                |
| 60         | 1       | 136             | 6                   | X <sub>5</sub> CX <sub>16</sub> CX <sub>4</sub> CX <sub>46</sub> CX <sub>12</sub> CX <sub>39</sub> CX <sub>8</sub>  | ML domain                           |
| 61         | 2       | 195             | 6                   | X <sub>6</sub> CX <sub>131</sub> CX <sub>16</sub> CX <sub>25</sub> CX <sub>4</sub> CX <sub>7</sub> C  | CRISP                               |
| 62         | 1       | 355             | 4                   | X <sub>33</sub> CX <sub>166</sub> CX <sub>11</sub> CX <sub>104</sub> CX <sub>37</sub> C   | Hyaluronidase                       |

Z, pyroglutamic acid; #, C-terminal amidation.

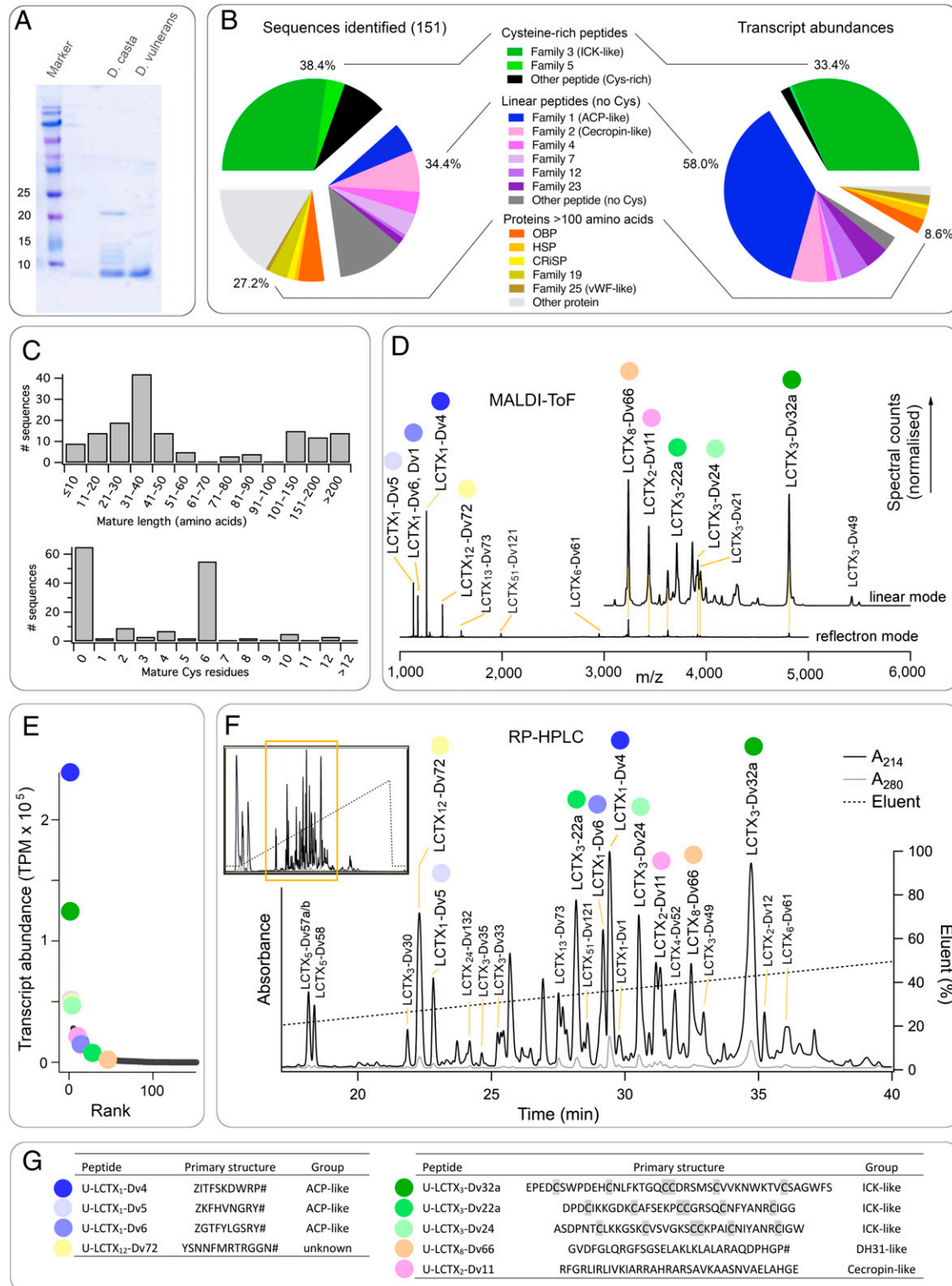


**Fig. 2.** Peptide-rich venom of *D. vulnerans*. (A) Sodium dodecyl sulfate polyacrylamide gel electrophoresis of *D. casta* and *D. vulnerans* venom showing abundant peptides <10 kDa. (B) Numbers (Left) and transcript abundances (Right) of amino acid sequences detected in venom. Note the high abundance of toxin families with sequence similarity to ACP, cecropins, and ICKs (Families 1, 2, and 3, respectively). (C, Upper) Length of mature polypeptides in venom; note large number of peptides with 31 to 40 residues. (C, Lower) Number of cysteines in mature toxin sequences; most toxins have either zero or six cysteine residues. (D) MALDI-ToF mass spectra of *D. vulnerans* venom. The Upper shows a spectrum obtained in linear mode (which gives better signal at higher *m/z*), while the Lower is a spectrum obtained in reflectron positive mode (which gives better mass resolution). (E) Transcript abundance plotted against transcript abundance rank for the 151 toxin-encoding transcripts detected. (F) Chromatogram from C18 RP-HPLC fractionation of ~0.5 mg *D. vulnerans* venom. The Inset shows the entire chromatogram and the main figure a magnification of the region indicated by the orange box in the Inset. (G) Primary structure of selected highly abundant venom peptides. Z, pyroglutamic acid; #, C-terminal amidation.



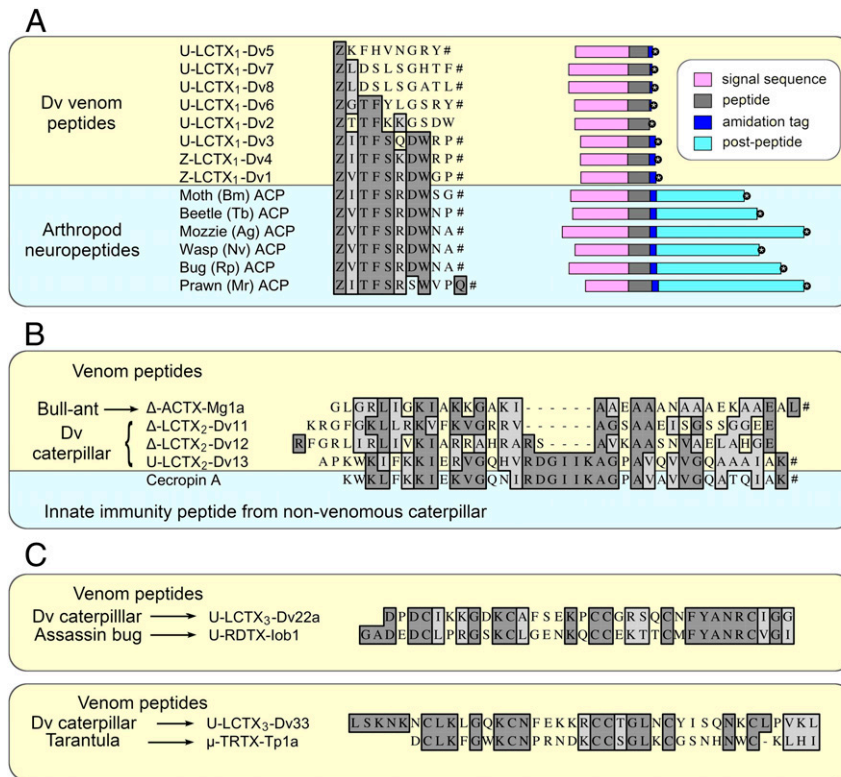


**Fig. 3.** Similarity of the most abundant venom peptide families to known peptides. (A) The *Left* shows an alignment of *D. vulnerans* Family 1 venom peptides with endogenous ACP neuropeptides from insects and crustaceans (51, 78). Z, pyroglutamic acid; #, C-terminal amidation. Dv, *D. vulnerans*; Bm, silkworm *Bombyx mori*; Tc, red flour beetle *Tribolium castaneum*; Ag, mosquito *Anopheles gambiae*; Nv, wasp *Nasonia vitripennis*; Rp, kissing bug *Rhodnius prolixus*; Mr, giant freshwater prawn *Macrobrachium rosenbergii*. Boxed residues in dark and light gray indicate identity and similarity, respectively, with the consensus of endogenous neurohormone sequences. The architecture of the precursors (translated ORFs) for each peptide is shown on the *Right*. Note the C-terminal propeptide region (light blue) is universally present in the precursors of endogenous neuropeptides and universally absent in the precursors of venom peptides. Black-circled stars indicate stop codons. (B) Alignment of *D. vulnerans* Family 2 peptides with the ant venom peptide Mg1a and the innate immune peptide cecropin A from the moth *H. cecropia* (79). (C) Alignment of two *D. vulnerans* Family 3 venom peptides with previously reported peptides. (Upper) Similarity of Dv22a to peptide U-RDTX-lob1 from venom of the assassin bug *Isyndus obscurus* (80). (Lower) Similarity of Dv33 with  $\mu$ -TRTX-Tp1a, a modulator of voltage-gated sodium channels from venom of the tarantula *Thrixopelma pruriens* (81).

Peptides in Family 3 contain six cysteine residues in an arrangement consistent with the inhibitor cystine knot (ICK) fold. ICKs occur widely in nonvenomous invertebrates and plants and have been convergently recruited into the venoms of diverse taxa including arachnids, cone snails, assassin bugs, robber flies, and centipedes (31–34). Venom ICKs have a broad range of bioactivities but are most commonly modulators of ion channels. *D. vulnerans* venom contains 41 putative ICK toxins ranging from 28 to 51 residues in length (SI Appendix, Fig. S2). Some are similar to assassin bug venom peptides (e.g., U-LCTX<sub>3</sub>-Dv22a; E < 10<sup>-6</sup> BLAST homology to Iob1, a venom peptide of the assassin bug *Isyndus obscurus*), while others are more similar to spider venom toxins (e.g., U-LCTX<sub>3</sub>-Dv33; BLAST E < 0.05 to  $\mu$ -TRTX-Tp1a from the venom of the tarantula *Thrixopelma pruriens*) (Fig. 3C). However, the vast majority of Family 3 peptides have no homology to known peptides. Two of the most abundant putative ICK toxins in *D. vulnerans* venom are U-LCTX<sub>3</sub>-Dv32a (EPEDCSWP-DEHCNLFKGTGCCDRSMSCVVKWKTVCAGWFS) and U-LCTX<sub>3</sub>-Dv24a (ASDPNTCLKKGSKCVSVGKSCCKPAICNIY-ANRCIGW) (Fig. 2).

**Rich Diversity of Venom Toxins.** *D. vulnerans* venom contains a rich diversity of other peptides and proteins with potentially novel structural and functional properties (Fig. 2 and Dataset S1). In addition to the three major families described above, abundant venom peptides that belong to single-member families include U-LCTX<sub>12</sub>-Dv72 (YSNFMRTTRGGN-NH<sub>2</sub>), U-LCTX<sub>8</sub>-Dv66

(GVDFGLQRFSGSELAKLKLALARAQDPHGP-NH<sub>2</sub>) which is similar to calcitonin-like diuretic hormone 31 (DH<sub>31</sub>) (35), and a disulfide-rich peptide of unknown structure U-LCTX<sub>6</sub>-Dv61 (ISFDCSDKPPCCQNDPCCFDIGITTF). Overall, 26 of the 59 toxin families did not have detectable homology to known peptide sequences.

Additional disulfide-rich peptides include Kazal-domain peptides (Family 16), von Willebrand-domain peptides (Family 25), as well as peptides with unknown structures such as U-LCTX<sub>15</sub>-Dv77a (AKCLISVSLCPQQRKCVSFSKFPDGYKCVADCD-ECKALLK). An unusual case is the 8.6 kDa peptide U-LCTX<sub>10</sub>-68a, which has six cysteines and is similar to the disulfide-rich domain of low-density lipoprotein (LDL) receptor class A. In *D. vulnerans* venom, it occurs uniquely as a single domain but retains the key residues demonstrated to be responsible for binding both Ca<sup>2+</sup> and LDL (SI Appendix, Fig. S3A). U-LCTX<sub>18</sub>-82 is an 8.9 kDa peptide with 12 cysteine residues that is similar to fungal protease inhibitor-1 from the Indian silkworm *Antheraea mylitta* (36).

Some larger venom proteins were similar to those found in other animal venoms and can be inferred to have been recruited convergently in Limacodidae. These include CRISPs, the putative venom spreading factor hyaluronidase, a protein similar to honeybee venom acid phosphatase Api m 3, and odorant binding proteins similar to those reported to occur in the venoms of wasps and assassin bugs (34, 37). The venom also contained two proteins with similarity to the chloride transport modulator ion transport peptide/crustacean hyperglycemic hormone (ITP/CHH)

(38), which has been convergently recruited into the venom of spiders and centipedes (39). *D. vulnerans* venom Family 19 contained five proteins of ~12 kDa that are devoid of cysteine residues and which are similar to proteins found in venoms from assassin bugs and robber flies (many BLAST *E* values < 10<sup>-10</sup> to heteropteran venom Family 3 and asilid venom Family 11; see alignment in *SI Appendix, Fig. S3B*). We also detected a 12.8 kDa protein with 10 cysteine residues (Family 9) that is similar to the JAK/STAT pathway inhibitor Diedel (40).

*D. vulnerans* venom also contained proteins with homology to protein families that, to the best of our knowledge, have not previously been detected in animal venoms. For example, the venom contains three 21 kDa proteins that are similar (BLAST *E* < 10<sup>-10</sup>) to the intracellular neuronal protein calyculin, which has been implicated in Pavlovian learning in the squid *Doryteuthis pealeii* (41). *D. pealeii* calyculin binds Ca<sup>2+</sup> and guanosine-5'-triphosphate, increases membrane excitability by inhibiting voltage- and Ca<sup>2+</sup>-activated K<sup>+</sup> channels, and binds to and stimulates Ca<sup>2+</sup> release from the ryanodine receptor (41). Calyculin also occurs in arthropods, though its physiological role is poorly characterized (42). Unlike mollusk calyculins, *D. vulnerans* venom calyculins possess a secretion signal, lack threonine phosphorylation sites and disulfide bridges, and retain most of the EF-hand residues responsible for Ca<sup>2+</sup> binding (*SI Appendix, Fig. S3C*).

**Toxin Processing in the Limacodid Secretory Pathway.** The data we obtained on precursor and mature peptide primary structures provide insights into limacodid venom peptide processing. For example, the vast majority of detected venom peptides possess a secretion signal peptide (148 of 151 polypeptides with SignalP D-score > 0.45). This indicates that canonical secretion through the endoplasmic reticulum is the major pathway by which polypeptides are secreted into the lumen of the venom spine.

Most peptides are translated from ORFs with a simple arrangement encoding a signal peptide, mature peptide, and stop codon (*SI Appendix, Fig. S4A*). Other ORFs encode precursors with sequence tags that destine them to be posttranslationally modified (*SI Appendix, Fig. S4B*). Aside from disulfide bond formation, C-terminal amidation is the most common PTM in *D. vulnerans* venom, occurring in 31 polypeptides or 20.5% of the proteome. ORFs ending with a Gly, Gly-Lys, or Gly-Lys-Lys, or Gly-Arg-Lys preceding the stop codon have these tags removed, and the mature peptide is  $\alpha$ -amidated at the C-terminal residue (*SI Appendix, Fig. 4B*); U-LCTX<sub>3</sub>-Dv22, which ends in Gly-Gly, is apparently the only exception to this rule. These data are consistent with previous reports on the amidation of arthropod peptide hormones and venom toxins (30, 43, 44) but contrast with the scarcity of PTMs observed in venoms of reduviid insects (34, 45). The second most common PTM in *D. vulnerans* venom is cyclization of N-terminal glutamine to pyroglutamate, which occurs in 23 polypeptides or 15.2% of the proteome—apparently every case in which the encoded N-terminal residue is glutamine.

Some precursors undergo more complex processing (*SI Appendix, Fig. S4C*). For example, U-LCTX<sub>8</sub>-Dv66, which is similar to the insect neuropeptide calcitonin-like DH<sub>31</sub>, is produced from an ORF encoding a signal peptide, propeptide, and multiple copies of the mature peptide separated by short spacer regions that were not detected in the venom. These spacer regions begin with a Gly residue followed by the tetrabasic cleavage site Arg-Lys-Arg-Arg and end with a dibasic cleavage site Lys-Arg. The final copy of the peptide ends in Pro-Gly-Arg-Lys, which is processed to Pro-amide. The preceding copies of the peptide are also amidated, with their amidation tags apparently consisting of the Gly residue followed by the tetrabasic cleavage site.

Finally, some of the larger proteins detected in venom can be inferred by sequence similarity to be involved in posttranslational modification of venom components. One (U-LCTX<sub>41</sub>-Dv111) is a peptidylglycine  $\alpha$ -hydroxylating monooxygenase (PAM), an enzyme

essential for C-terminal amidation of arthropod neuropeptides (43, 44). Glutamyl cyclase, responsible for cyclizing N-terminal Gln residues to form pyroglutamate (46), was also detected. Angiotensin-converting enzyme (ACE), the chaperone Hsp20, and possibly other proteins detected in venom by MS, may also have roles in toxin maturation.

**Cecropin-like Peptides Are Responsible for the Painful Effects of Venom.** To identify pain-inducing molecules in *D. vulnerans* venom, we applied whole venom, venom fractions, and laboratory-produced versions of 13 venom peptides, to dissociated mouse dorsal root ganglion (DRG) neurons and monitored increases in intracellular Ca<sup>2+</sup> ([Ca<sup>2+</sup>]<sub>i</sub>). In this assay, increases in [Ca<sup>2+</sup>]<sub>i</sub> are used as a proxy for neuronal activation that would occur during nociception (47). The 13 laboratory-produced peptides were obtained by solid-phase peptide synthesis (SPPS) or heterologous expression using an *Escherichia coli* periplasmic expression system (48) and represent peptides detected in active fractions of venom, as well as peptides that are abundant in venom (Table 2 and *SI Appendix, Fig. S5*).

Application of whole venom (100  $\mu$ g/mL) to DRG neurons caused a rapid increase in [Ca<sup>2+</sup>]<sub>i</sub> (Fig. 4A and B and *SI Appendix, Fig. S6 A and B*). This effect was not blocked by preincubation of cells with 1  $\mu$ M tetrodotoxin (TTX), 100  $\mu$ M Cd<sup>2+</sup>, or 50  $\mu$ M Zn<sup>2+</sup>, indicating that it does not depend on TTX-sensitive voltage-gated sodium (Nav) or voltage-gated calcium (Ca<sub>v</sub>) channels (Fig. 4C and *SI Appendix, Fig. S6 C–E*). Removal of Ca<sup>2+</sup> from the extracellular medium abolished this response, indicating that the increase in [Ca<sup>2+</sup>]<sub>i</sub> is due to influx of extracellular Ca<sup>2+</sup> rather than release from intracellular stores. These data suggest that the dominant effect of whole venom is to increase the permeability of neuronal cell membranes to ions through a mechanism similar to pore or channel formation, although additional mechanisms might also contribute.

Applying fractions from C18 RP-HPLC separation of venom to DRG cells identified several early-eluting fractions (likely salts and small molecules) and a single later-eluting fraction (fraction 25, f25) that induced increases in [Ca<sup>2+</sup>]<sub>i</sub> (*SI Appendix, Fig. S7A*). LC-MS/MS and MALDI-TOF analysis revealed that f25 contained several peptides. Further fractionation of f25 using a more gradual RP-HPLC gradient revealed that only sub-fraction f25-17, which contained the cecropin-like U-LCTX<sub>2</sub>-Dv12 (RFGLRLIVKIARRAHRARSVAKASNVLAELAHGE) and U-LCTX<sub>7</sub>-Dv63 (VFSEFKKAFKGLFEKAANKYLH) was able to activate sensory neurons (*SI Appendix, Fig. S7 B–G*).

To investigate if these peptides could activate pain-sensing neurons, we applied synthetic versions of both peptides to DRG cultures. U-LCTX<sub>2</sub>-Dv12 caused robust Ca<sup>2+</sup> influx (Fig. 4C and *SI Appendix, Fig. S8*), whereas U-LCTX<sub>7</sub>-Dv63 had no effect. At a concentration of 10  $\mu$ M, U-LCTX<sub>2</sub>-Dv12 caused release of fluorescent dye from DRG cells, indicating lysis or formation of pores at the plasma membrane (*SI Appendix, Fig. S8A*). At 1  $\mu$ M concentration, calcium influx occurred without dye leakage, consistent with formation of a smaller pore or channel (*SI Appendix, Fig. S8B*). U-LCTX<sub>2</sub>-Dv12 closely recapitulated the effect of whole venom on DRGs, as it induced calcium influx that was not blocked by TTX or Cd<sup>2+</sup> but was dependent on Ca<sup>2+</sup> in the extracellular medium (Fig. 4C and *SI Appendix, Fig. S8 C–F*). We tested synthetic versions of 11 additional venom peptides, but only one, U-LCTX<sub>2</sub>-Dv11, activated DRG cells (Fig. 4C and *SI Appendix, Fig. S9*). U-LCTX<sub>2</sub>-Dv11 is a homolog of U-LCTX<sub>2</sub>-Dv12, with 45% sequence similarity. Intraplantar injection in mice of synthetic U-LCTX<sub>2</sub>-Dv11 and U-LCTX<sub>2</sub>-Dv12 (600 pmol in 20  $\mu$ L) induced immediate nociceptive behavior (Fig. 4D) that resolved within 5 min, a time course consistent with our experience with human envenomations by this species.

Our data indicate that Family 2 peptides in *D. vulnerans* venom are responsible for activation of sensory neurons in vitro and induction of pain in vivo. The finding that this neuronal

**Table 2. Peptides produced in this study and their observed bioactivities**

| Name                       | Homology         | Amino acid sequence                      | DRG assay     | Insecticidal              |                            | Antimicrobial       | Nematocidal EC <sub>50</sub> (μM) |
|----------------------------|------------------|--|---------------|---------------------------|----------------------------|---------------------|-----------------------------------|
|                            |                  |  |               | EC <sub>50</sub> (nmol/g) | ACPR EC <sub>50</sub> (nM) | (lowest MIC, μg/mL) |                                   |
| U-LCTX <sub>1</sub> -Dv5   | ACP              | ZKFHVNGRY#                               | None          | >50                       | >10,000                    | nd                  | nd                                |
| Z-LCTX <sub>1</sub> -Dv1   | ACP              | ZVTFSRDWGP#                              | None          | >50                       | <b>0.55</b>                | nd                  | nd                                |
| Z-LCTX <sub>1</sub> -Dv4   | ACP              | ZITFSKDWRP#                              | None          | >50                       | <b>3.07</b>                | nd                  | nd                                |
| U-LCTX <sub>12</sub> -Dv72 | ?                | YSNNFMRTGGN#                             | None          | >50                       | nd                         | None                | >100                              |
| U-LCTX <sub>13</sub> -Dv73 | ?                | NGPQGSDDRNWIRL#                          | None          | >50                       | nd                         | None                | 94.5                              |
| U-LCTX <sub>14</sub> -Dv74 | ?                | ACKGKKCPPTGFVGMR#                        | None          | >50                       | nd                         | None                | >100                              |
| U-LCTX <sub>7</sub> -Dv63  | ?                | VFSEFKKAFKGLFEKAANKYLH                   | None          | <b>10.27</b>              | nd                         | None                | 41.3                              |
| U-LCTX <sub>6</sub> -Dv61  | ?                | ISFDCSDKPPCCQNDPGCCFDIGITTF              | None          | >50                       | nd                         | None                | >100                              |
| U-LCTX <sub>8</sub> -Dv66  | DH <sub>31</sub> | GVDFGLQRGFGSELAKLKLALARAQDPHGP#          | None          | >50                       | nd                         | None                | >100                              |
| Δ-LCTX <sub>2</sub> -Dv11  | Cecropin         | KRGFGKLLRKVFKVRRVAGSAAEISGSSGGEE         | <b>Strong</b> | <b>4.73</b>               | nd                         | <b>&lt;0.25*</b>    | 30.5                              |
| U-LCTX <sub>3</sub> -Dv21  | ICK              | ASDPNKCLKKGSKCVSVGKPCCKPATCNIYANRCIGW    | None          | >50                       | nd                         | nd                  | 22.1                              |
| Δ-LCTX <sub>2</sub> -Dv12  | Cecropin         | RFGRLIRLIVKIARRAHRARSVAKAASNVAELAHGE     | <b>Strong</b> | <b>4.01</b>               | nd                         | <b>&lt;0.25†</b>    | 24.5                              |
| U-LCTX <sub>3</sub> -Dv33  | ICK              | GLSKNKNCCLKGQKCNFEKKRCCTGLNCYISQNKCLPVKL | None          | >50                       | nd                         | None                | <b>2.6</b>                        |

Z, pyroglutamic acid; #, C-terminal amidation; nd, not determined. Results of note are shown in bold font. Note that recombinant Dv33 carries an N-terminal Gly residue not present in the natural peptide.

\**A. baumannii*.

†*A. baumannii*, *S. aureus*, and *C. neoformans* var. *gubii*.

activation does not depend on Na<sub>v</sub> or Ca<sub>v</sub> channels, along with the structural similarity of these peptides to both aculeatoxins and cecropins (Fig. 3B), suggest that they function by forming ion-permeable pores in lipid bilayers. Subsequently, we refer to them with a Δ prefix to indicate this mode of action (26).

**Abundant Neurohormone-like Peptides Potently Activate Insect ACPRs.** Family 1 peptides are among the most abundant in *D. vulnerans* venom (Fig. 2) and show similarity to the endogenous insect ACP neuropeptide. We applied three synthetic *D. vulnerans* Family 1 venom peptides to the ACP receptor (ACPR) from the mosquito *Aedes aegypti* (49, 50) and found that two of them (hereafter indicated with prefix Z) activated the receptor with picomolar potency (Fig. 4E) while having no activity on receptors of the closely related neuropeptides adipokinetic hormone and corazonin (51, 52). The potency of Z-LCTX<sub>1</sub>-Dv1 and Z-LCTX<sub>1</sub>-Dv4 on the *A. aegypti* ACPR (EC<sub>50</sub> of 0.55 and 3.07 nM, respectively) is comparable to the endogenous ligand (EC<sub>50</sub> 0.62 nM), whereas U-LCTX<sub>1</sub>-Dv5 had no effect. Injection of these three synthetic peptides into crickets (*Acheta domesticus*) did not reveal any observable effects.

**Insecticidal, Antimicrobial, and Nematocidal Effects of Venom Peptides.** Arthropod venoms contain numerous insecticidal, antimicrobial, and antiparasitic molecules (53–55), and cecropins and their synthetic derivatives have been extensively explored for their antimicrobial and antiparasitic activities (56, 57). We therefore hypothesized that the cecropin-like venom peptides (Family 2), and perhaps other *D. vulnerans* venom peptides, might display activity against microbes, multicellular pathogens, or insects.

To test for insecticidal activity, we injected whole venom and synthetic venom peptides into fruit flies. Injection of ~50 μg/g whole venom (50 nL at ~1 mg/mL) into *Drosophila melanogaster* did not induce death or complete paralysis, but caused noticeable alterations in motor behavior characterized by a slow, jerky gait. These effects were nonlethal and reversible over 24 h. Injection of the cecropin-like peptides Δ-LCTX<sub>2</sub>-Dv12 and Δ-LCTX<sub>2</sub>-Dv11, and U-LCTX<sub>7</sub>-Dv63, induced complete paralysis or death of *D. melanogaster*. At the highest dose tested (50 nmol/g), these peptides caused sudden wing beating followed by complete immobility (as measured using a *D. melanogaster* climbing assay; Fig. 4F). In the case of Δ-LCTX<sub>2</sub>-Dv12 and U-LCTX<sub>7</sub>-Dv63, flies never recovered after paralysis, but paralysis induced by 50 nmol/g Δ-LCTX<sub>2</sub>-Dv11 was partially

reversible after 24 h. Injection of lower doses of these peptides produced weaker effects, transitioning through reversible paralysis to little or no discernible effect for doses ≤0.5 nmol/g. The EP<sub>50</sub> values for paralysis of *D. melanogaster* by injection of Δ-LCTX<sub>2</sub>-Dv11, Δ-LCTX<sub>2</sub>-Dv12, and U-LCTX<sub>7</sub>-Dv63 were 4.73, 4.01, and 10.27 nmol/g, respectively (Fig. 4F). These effects are similar to those induced in the same assay by the ant venom peptide Δ-ACTX-Mg1a (Fig. 3B), which shares many structural features and is thought to act via the same mechanism of membrane disruption (30). Injection of the 10 other synthetic venom peptides did not produce any noticeable effect. Thus, Family 2 venom peptides may protect limacodid caterpillars from both vertebrate and insect predators.

To test if *D. vulnerans* venom peptides had antimicrobial activity, we submitted synthetic and recombinant venom peptides to the Community for Antimicrobial Drug Discovery (CO-ADD), where they were tested for their ability to inhibit the growth of a range of Gram-negative and Gram-positive bacteria and fungi, as well as their ability to kill or lyse human cells. The cecropin-like Family 2 peptides showed strong antibacterial activity, with Δ-LCTX<sub>2</sub>-Dv12 inhibiting the growth of six of the seven microbes tested with minimum inhibitory concentrations (MICs) <32 μM (Table 2 and SI Appendix, Table S1). For the Gram-positive *Staphylococcus aureus*, Gram-negative *Acinetobacter baumannii*, and the invasive fungus *Cryptococcus neoformans* var. *gubii*, the MIC of these peptides was lower than the lowest concentration tested, 0.25 μM. Δ-LCTX<sub>2</sub>-Dv11 showed comparable activity against *A. baumannii* and lesser activity against *S. aureus*. Δ-LCTX<sub>2</sub>-Dv12 was found to be cytotoxic and hemolytic at concentrations close to 19 μM, whereas Dv11 was not cytotoxic up to >32 μM. No peptide was active against the yeast *Candida albicans*, and venom peptides other than Family 2 peptides did not have any effect on microbial growth. These data indicate that the cecropin-like venom peptides have antimicrobial activities, as reported for nonvenom cecropins.

Previous studies of the antiparasitic activity of cecropins have focused exclusively on protozoan parasites (malaria, leishmania, and trypanosomes) (56, 58). We tested the ability of *D. vulnerans* synthetic venom peptides, including cecropin-like and other peptides, to inhibit development of larvae of both drug-susceptible and drug-resistant isolates of the nematode *Haemonchus contortus*, a gastrointestinal parasite of sheep, using an assay that is also a model for anthelmintic activity relevant to animal and human health (59).



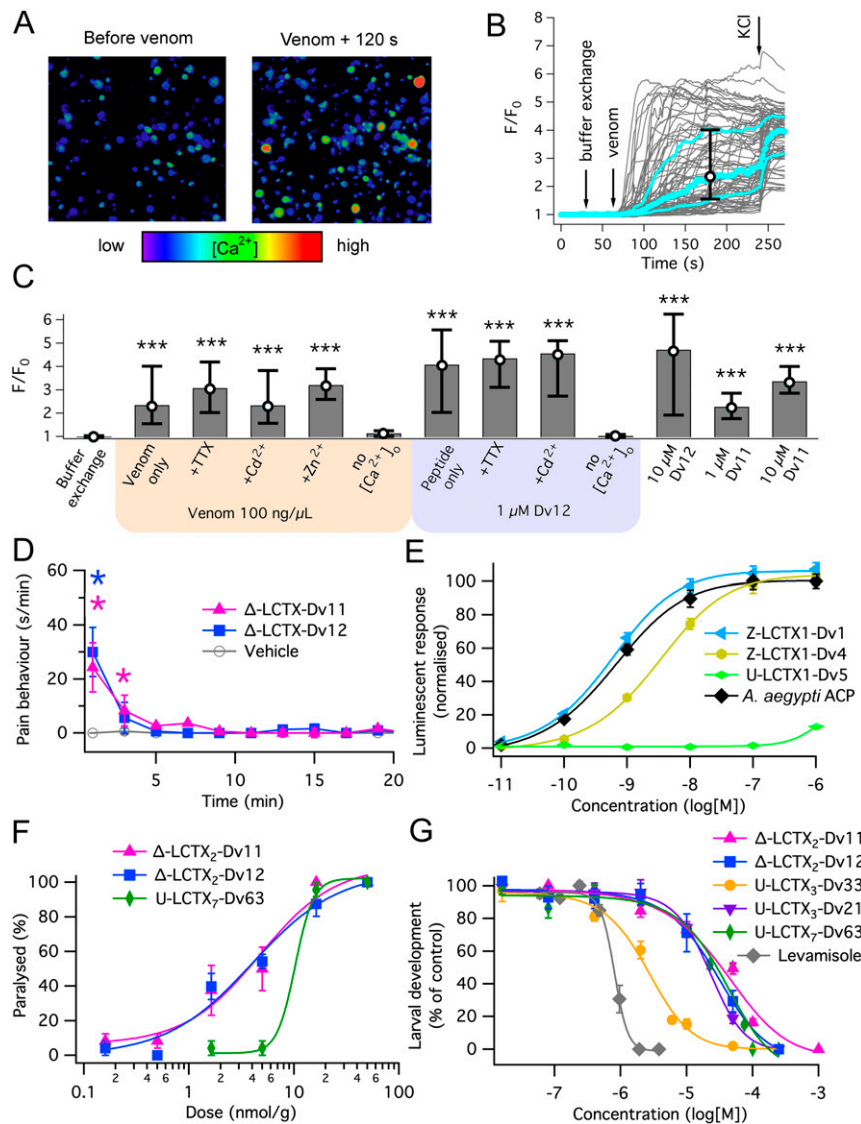


**Fig. 4.** Bioactivity of venom and venom peptides. (A) Photomicrograph of DRG cells before and 120 s after application of 100 ng/ $\mu$ L venom. (B) Resulting calcium influx measured as an increase in fluorescence relative to baseline ( $F/F_0$ ). Each gray trace corresponds to one cell. The thick light blue trace shows the median  $F/F_0$  response, and the thinner light blue lines show the first and third quartile values ( $Q_1$  and  $Q_3$ ). The median,  $Q_1$ , and  $Q_3$  values 120 s after venom addition (at 180 s in this trace) were recorded for comparison to other experiments. (C) Comparison of  $F/F_0$  values of populations of cells, 120 s after exposure to venom or synthetic venom peptides. Hollow points show the median and error bars show  $Q_1$  and  $Q_3$ . \*\*\*, highly significant ( $P < 10^{-10}$ ) difference compared to buffer exchange and  $Ca^{2+}$ -free conditions, by Kruskal–Wallis test. ns, not significant by Kruskal–Wallis compared to buffer exchange and  $Ca^{2+}$ -free conditions. (D) Nocifensive behavior in mice after intraplantar injection of cecropin-like venom peptides. Stars indicate statistical significance of  $P < 0.05$  (Student's  $t$  test compared to vehicle). Error bars in D–G indicate SEMs. (E) Activation of the *Aedes aegypti* ACP by subnanomolar concentrations of ACP-like venom peptides Z-LCTX<sub>1</sub>-Dv1 and Z-LCTX<sub>1</sub>-Dv4. (F) Insecticidal activity of three venom peptides, measured as inhibition of *D. melanogaster* climbing response due to death or paralysis. (G) Ability of peptides to interfere with larval development of the parasitic nematode *H. contortus*. Each point represents three repeats of duplicate assays for peptides or two repeats for the commercial anthelmintic levamisole.

We found that micromolar concentrations of the cecropin-like peptides  $\Delta$ -LCTX<sub>2</sub>-Dv12 and  $\Delta$ -LCTX<sub>2</sub>-Dv11 inhibited development of the drug-susceptible Kirby isolate ( $IC_{50}$  values of 24.5 and 30.5  $\mu$ M, respectively; Fig. 4G and *SI Appendix, Table S2*). Surprisingly, the Family 3 ICK-like peptides, which did not show pain-inducing or insecticidal properties, possessed the strongest anthelmintic activity. Recombinant U-LCTX<sub>3</sub>-Dv33 inhibited *H. contortus* development at low micromolar concentrations ( $IC_{50}$  2.6  $\mu$ M), which is only sixfold higher than that measured for the commercial anthelmintic levamisole ( $IC_{50}$  0.42  $\mu$ M for the drug-susceptible Kirby isolate). U-LCTX<sub>3</sub>-Dv21, U-LCTX<sub>7</sub>-Dv63, and U-LCTX<sub>13</sub>-Dv73 also showed moderate anthelmintic activity with  $IC_{50}$  values of 20 to 100  $\mu$ M, while the other four peptides did not have

appreciable effects on larval development. Results obtained using the drug-resistant isolate MPL-R were similar, indicating no cross-resistance exists toward the peptides (overlap of 95% CIs between  $IC_{50}$  for the Kirby and MPL-R isolates for each peptide), in contrast to the significant resistances shown by the MPL-R isolate to commercial anthelmintics (*SI Appendix, Table S2*).

## Discussion

We report a detailed account of the anatomy of venom production, the composition of venom, and bioactivity of peptides underlying pain induction by venoms of the Limacodidae. *D. vulnerans* venom contains a diverse assortment of peptides, and we demonstrate that many of these are potentially bioactive.

Although we named individual peptides in accordance with rational toxin nomenclature (26), we furthermore propose the common name of “vulnericins” for venom peptides from *D. vulnerans*, consistent with previously described bioactive peptides discovered in Lepidoptera such as cecropin (from the cecropia moth *Hyalophora cecropia*). Representatives of Family 1 vulnericins were shown to activate insect GPCRs with picomolar efficacy; Family 2 vulnericins were shown to disrupt cell membranes and thereby induce pain when injected into vertebrates, as well as killing insects, microbes, and nematodes; and Family 3 vulnericins displayed antiparasitic effects albeit through unknown pharmacology. Since the name vulnericin can be interpreted etymologically to mean “pain-causing substance,” it is especially appropriate for those peptides shown to induce pain. Overall, our results provide support for current theories of venom evolution, including the convergent recruitment of endogenous peptides and proteins with innate toxin-like properties in multiple animal groups (4); and toxin divergence through the duplication and neofunctionalization of toxin-encoding genes (5, 60). Below, we discuss the evolution of venom use in Limacodidae in more detail.

**Anatomy Underlying Venom Production.** A variety of anatomical structures associated with venom production and delivery have been described in caterpillars (61, 62). Some of the reported variation is due to differences between taxonomic groups. For example, in some larval Erebidae and Thaumetopoeinae, urticating spicules, which are likely modified hairs containing internal canals filled with irritative or pain-causing venoms, are the dominant structures (63). Although limacodid caterpillars possess similar structures (61), we obtained venom from the much larger and sturdier hollow venom spines. Our data suggest that these spines are evaginations of the body wall itself, as previously proposed for venom spines of the Limacodidae, Megalopygidae, and Saturniidae (62, 64), rather than being derived from hairs (61). In Saturniidae, the location of the venom-secreting cells is less well characterized, and some spines may inject haemolymph rather than a specialized venom (62). Our data are consistent with previous reports that ascribe venom secretion in Limacodidae and Megalopygidae to the large cell at the base of each spine (61, 64). This observation is consistent with the descent of diverse venomous zygaenoids from a shared venomous ancestor with subsequent loss of venom use in some groups (12). However, we cannot rule out that venom use evolved multiple times in Zygaenoidea, possibly from similar molecular and anatomical precursors. Further information on the production and composition of nonlimacodid zygaenoid venoms is required to investigate these possibilities.

**Recruitment and Radiation of Venom Toxins.** *D. vulnerans* venom was shown to contain a diverse assortment of polypeptides, the most abundant of which are <10 kDa in mass. This finding clearly indicates convergent evolution between limacodids and many other animal groups with peptide-rich venoms such as arachnids, hymenopteran insects, and cone snails (8). In contrast, venoms including those of some saturniid caterpillars, heteropteran insects, robber flies, jellyfish, and centipedes, feature abundant and functionally important proteins >10 kDa (1, 33, 34, 45, 65–67). The evolutionary drivers of toxin mass distribution across the tree of life remain to be elucidated.

While venoms devoted to defensive use are sometimes suggested to be simple in composition compared to venoms used for predation or multiple ecological interactions (7, 30, 68), we found the defensive venom of *D. vulnerans* to be highly complex. The venom contains an abundance of both cysteine-rich peptides and linear peptides, each of which accounted for approximately half of the peptides detected. The profusion of linear peptides, including cationic/amphipathic peptides such as the cecropin-like Family 2, demonstrates convergence with hymenopteran venoms, whereas the large number of disulfide-rich knottins shows convergence with

arachnid venoms. Some toxin families, including neurohormones, knottins, hyaluronidase, CRiSPs, acid phosphatase, ITP/CHH, Kazal domain peptides, and others, have been recruited into both limacodid and other animal venoms. These data provide further support for the hypothesis that proteinaceous toxins frequently originate from endogenous peptides and proteins with inherently toxin-like pharmacokinetic properties (4). A prerequisite for this theory is the conservation of multiple groups of toxin-like polypeptides in the endogenous proteomes of nonvenomous animals. Signaling molecules such as neuropeptides, which are used by an animal to induce a change in its own physiology, are one class of suitable peptides from which the limacodid ACP-, ITP/CHH-, and DH<sub>31</sub>-like venom toxins have been recruited, similar to the recruitment of neurohormones into venoms of wasps, arachnids, sea anemones, and cone snails (39, 69–71). Another class are immune system peptides, which provide defense against pathogens and parasites, and from this class limacodids have recruited cecropin-like venom toxins and probably also ICK- and Diedel-like toxins. The co-option of immune system peptides and proteins into venom has previously been noted to contribute to venom evolution, notably among arachnids and snakes (31, 72, 73). Other toxins (e.g., those with similarity to calyctoxins) have a role in the nervous system, at least in mollusks (41). In insects, their role is poorly characterized, but they have been adapted as secreted proteins in *D. vulnerans* and some hemipteran insects (42). Finally, many endogenous toxin-like proteins, such as acid phosphatase and hyaluronidase, have multiple physiological roles in nonvenomous animals. Presumably, there are many different toxin-like polypeptides in any given nonvenomous animal, and a subset of these are recruited as venom toxins during the evolution of venom use.

After recruitment for venom production, toxin-encoding genes have frequently been hypothesized to undergo duplication events followed by conservation of one daughter gene for the original nonvenom role and neofunctionalization of others for venom production (4, 5, 60). In contrast, some studies have found co-option of single-copy genes to be evolutionary processes of similar or greater importance for toxin recruitment (74, 75). In *D. vulnerans*, we observed patterns strongly suggestive of gene duplication and neofunctionalization in several gene families. The striking sequence divergence and changes in precursor architecture observed in Family 1 toxins strongly suggest duplication and neofunctionalization, although it is not clear if *D. vulnerans* retains an endogenous ACP/ACPR signaling system. The occurrence of multiple Family 2 peptides, one of which closely resembles nonvenom cecropins in sequence (U-LCTX-Dv13) while others ( $\Delta$ -LCTX-Dv11 and -Dv12) are more divergent in sequence, more abundant in venom, and responsible for inducing nociception, also probably reflects this pattern. While our findings support the importance of gene duplication and neofunctionalization in the evolution of limacodid venom toxins, it cannot inform us about their relative importance compared to other evolutionary processes. Such a comparison would require genomic data to distinguish products of different gene loci from allelic variants.

**Bioactivity of Venom Components.** A major finding of this work is that the cecropin-like Family 2 vulnericins activate mammalian sensory neurons and cause nociceptive behaviors in mice through a mechanism resembling pore or channel formation in cell membranes. Consistent with this proposed mechanism of generalized membrane disruption, Family 2 vulnericins possess antimicrobial, nematocidal, and insecticidal properties. Since these peptides induce nonspecific membrane disruption and pain, they are unlikely to represent clinically useful antimicrobials, but this finding is nevertheless informative from an evolutionary perspective, as it demonstrates that innate immunity peptides such as cecropins can be adapted to function as pain-inducing defensive venom peptides.

If the composition of *D. vulnerans* venom is optimized to confer a fitness advantage to the caterpillars that produce it, it displays several features that are highly enigmatic. Most strikingly, the

pain-inducing cecropin-like Family 2 vulnericins make up only a small fraction of the venom compared to ACP-like Family 1 peptides and ICK-like Family 3 peptides (6.4% compared to 37.2% and 31.4% of toxin-encoding transcripts, respectively). Family 1 peptides were found to be potent agonists of insect ACPRs, but none of the Family 1 or Family 3 peptides were active on either vertebrate cells or when injected into insects. For the ICK-like Family 3 peptides, we anticipate that more detailed electrophysiological studies may reveal ion channel modulating activities that contribute to nociception or other venom functions. Since the normal physiological role of the ACP/ACPR signaling system is yet to be determined (50), it is unclear how ACP-like toxins might confer a fitness advantage to *D. vulnerans*. What we can infer is as follows: First, the duplication of ACP-like toxin genes combined with the high abundance of these toxins in venom suggests that their presence in venom has been selected for. Second, the fact that they are highly specific ligands for a particular insect GPCR suggests that the ecological interaction in which they confer a fitness advantage occurs between *D. vulnerans* and another insect. The important ecological interaction is currently unknown, but we hypothesize it may be 1) ACPR activation playing a role in nociception, or learnt avoidance of nociception, in insect predators; 2) activation of ACPR protecting caterpillars from parasitization by tachinid flies or wasps, a frequently reported event that leads to the death of the caterpillar (76); or 3) activation of ACPR conferring an advantage during competition between *D. vulnerans* and other leaf eaters for food resources. We are currently investigating these hypotheses, which may also reveal the normal physiological role of ACP/ACPR signaling.

An unexpected outcome of this study was the finding that the ICK-like Family 3 vulnericin U-LCTX<sub>3</sub>-Dv33 inhibits larval development of the nematode *H. contortus*. Since limacodid venoms are presumably not applied to nematodes or other helminths in nature, it is unclear if this activity reflects a useful adaptation on the part of limacodid caterpillars (e.g., by modulation of a specific invertebrate ion channel or signaling cascade that confers an advantage in some natural context). Alternatively, it might simply reflect the fact that complex peptide-rich venoms also represent chemical libraries containing diverse pharmacologies (8). In any case, we found that the ICK-like Family 3 vulnericins do not possess obvious cytolytic, pain-inducing, or other deleterious effects that would preclude their use as veterinary medicines. As helminths comprise the largest group of neglected tropical diseases and remain one of the biggest threats to veterinary medicine (77), these findings suggest that caterpillar venoms represent a novel resource for anthelmintic discovery.

**Summary.** We report a detailed overview of the venom system of a limacodid caterpillar, which has evolved independently to previously studied venoms. The venom is dominated by peptides

and is very complex in composition. Cecropin-like Family 2 vulnericins appear to be key mediators of the pain induced after limacodid envenomations of mammals and illustrate a viable evolutionary path for the recruitment of immune system peptides that target cell membranes as defensive venom toxins. Other peptides displayed potent activity on an insect GPCR and arresting the growth and development of parasites, but further work is required to understand the selection pressures responsible for recruiting these pharmacologies into venom. Our results support the convergent recruitment of endogenous toxin-like polypeptides, and duplication and neofunctionalization of toxin-encoding genes, as important processes underpinning the evolution of venom use. This study provides insights into the biology and evolution of lepidopteran defensive adaptations, as well as highlighting the Limacodidae as a rich source of bioactive peptides from which molecules with novel pharmacologies might be isolated.

## Materials and Methods

Detailed materials and methods are provided in *SI Appendix, Supplementary Methods*. In brief, light microscopy and  $\mu$ -CT of fixed tissues were used to investigate the structure of the venom apparatus. RNA-Seq of the venom scoli combined with bottom-up and top-down mass spectrometry (MS) of expelled venom were used to resolve a venom proteome. Functional testing was carried out on venom fractions separated by RP-HPLC as well as major peptides produced by SPPS and heterologous expression. Functional assays included calcium imaging of DRGs and cells expressing ACPR, and insecticidal, antimicrobial, and antinematocidal assays. Two peptides were also tested for their ability to induce pain-like behavior after intraplantar injection into mice.

**Data Availability.** The raw sequencing reads used in this project are available in fastq format from the National Center for Biotechnology Information (NCBI) Sequence Read Archive (BioProject ID [PRJNA672259](https://www.ncbi.nlm.nih.gov/bioproject/PRJNA672259)) and the assembled contigs from the Transcriptome Shotgun Assembly database (accession no. [GWVX00000000](https://www.ncbi.nlm.nih.gov/tx/GWVX00000000)). MS data are available from ProteomeXchange Consortium (PRIDE ID [PXD022400](https://www.ebi.ac.uk/pride/archive/projects/PXD022400)). Venom polypeptides and their encoding ORFs are available from GenBank (accession nos. [MW182018](https://www.ncbi.nlm.nih.gov/nuccore/MW182018)–[MW182168](https://www.ncbi.nlm.nih.gov/nuccore/MW182168)).

**ACKNOWLEDGMENTS.** We thank Alun Jones for MS support, Angelika Christ and Tim Bruxner from the Institute for Molecular Bioscience Sequencing Facility for performing RNA-Seq experiments, Angela Ruffell from the Commonwealth Scientific and Industrial Research Organisation Division of Agriculture and Food for assistance with *H. contortus* egg isolation, and Ian MacMillan and Mt. Gravatt Environment Group for use of photographs. Antimicrobial screening was performed by CO-ADD, funded by the Wellcome Trust (UK) and The University of Queensland (Australia). We acknowledge funding from The University of Queensland (Postdoctoral Fellowship and Early Career Researcher Grant UQECR1946597 to A.A.W.), Australian Research Council (ARC) (Discovery Project DP200102867 to A.A.W.; Discovery Project DP190103787 to S.D.R., I.V., and G.F.K.; and ARC Future Fellowship FT160100055 awarded to C.I.S.), Australian National Health and Medical Research Council (Principal Research Fellowship APP1136889 to G.F.K.), Natural Sciences and Engineering Research Council of Canada (Discovery Grant RGPIN-2018-05841 to J.-P.V.P.), and the Westpac Bicentennial Foundation (Westpac Future Leaders Scholarship to S.A.N.).

- L. C. Carrijo-Carvalho, A. M. Chudzinski-Tavassi, The venom of the *Lonomia* caterpillar: An overview. *Toxicon* **49**, 741–757 (2007).
- A. A. Walker *et al.*, Entomo-venomics: The evolution, biology and biochemistry of insect venoms. *Toxicon* **154**, 15–27 (2018).
- A. Y. Kawahara *et al.*, Phylogenomics reveals the evolutionary timing and pattern of butterflies and moths. *Proc. Natl. Acad. Sci. U.S.A.* **116**, 22657–22663 (2019).
- B. G. Fry *et al.*, The toxicogenomic multiverse: Convergent recruitment of proteins into animal venoms. *Annu. Rev. Genomics Hum. Genet.* **10**, 483–511 (2009).
- E. S. W. Wong, K. Belov, Venom evolution through gene duplications. *Gene* **496**, 1–7 (2012).
- A. A. Walker, The evolutionary dynamics of venom toxins made by insects and other animals. *Biochem. Soc. Trans.* **48**, 1353–1365 (2020).
- V. Schendel, L. D. Rash, R. A. Jenner, E. A. B. Undheim, The diversity of venom: The importance of behavior and venom system morphology in understanding its ecology and evolution. *Toxins (Basel)* **11**, 666 (2019).
- G. F. King, *Venoms to Drugs: Venom as a Source for the Development of Human Therapeutics* (Royal Society of Chemistry, Cambridge, UK, 2015).
- M. E. Epstein, Revision and phylogeny of the Limacodid-group families, with evolutionary studies on slug caterpillars (Lepidoptera: Zygaenoidea). *Smithson. Contrib. Zool.* **582**, 1–102 (1996).
- J. M. Zaspel, S. J. Weller, M. E. Epstein, Origin of the hungry caterpillar: Evolution of fasting in slug moths (Insecta: Lepidoptera: Limacodidae). *Mol. Phylogenet. Evol.* **94**, 827–832 (2016).
- C. R. Balit, M. J. Geary, R. C. Russell, G. K. Isbister, Prospective study of definite caterpillar exposures. *Toxicon* **42**, 657–662 (2003).
- Y.-C. Lin, R.-J. Lin, M. F. Braby, Y.-F. Hsu, Evolution and losses of spines in slug caterpillars (Lepidoptera: Limacodidae). *Ecol. Evol.* **9**, 9827–9840 (2019).
- S. M. Murphy, S. M. Leahy, L. S. Williams, J. T. Lill, Stinging spines protect slug caterpillars (Limacodidae) from multiple generalist predators. *Behav. Ecol.* **21**, 153–160 (2010).
- F. Trébouët, U. H. Reichard, N. Pinkaew, S. Malaivijitnond, Extractive foraging of toxic caterpillars in wild northern pig-tailed macaques (*Macaca leonina*). *Primates* **59**, 185–196 (2018).
- S. Pentzold *et al.*, Lepidopteran defence droplets—A composite physical and chemical weapon against potential predators. *Sci. Rep.* **6**, 22407 (2016).
- F. Walker, *List of the Specimens of Lepidopterous Insects in the Collection of the British Museum, Part XXXII: Supplement: Part 2* (British Museum, Natural History, London, 1865).
- F. Kawamoto, Studies on the venomous spicules and spines of moth caterpillars: III. Scanning electron microscopic examination of spines and spicules of the slug moth caterpillar, *Parasa consocia*, and some properties of pain-producing substances in their venoms. *Jap. J. Sanit. Zool.* **29**, 185–196 (1978).



18. J. W. Lewin, *Natural History of Lepidopterous Insects of New South Wales* (Thomas Lewin, London, 1805).
19. A. A. Walker, S. D. Robinson, B. F. Hamilton, E. A. B. Undheim, G. F. King, Deadly proteomes: A practical guide to proteotranscriptomics of animal venoms. *Proteomics* **20**, e1900324 (2020).
20. B. J. Haas *et al.*, *De novo* transcript sequence reconstruction from RNA-seq using the Trinity platform for reference generation and analysis. *Nat. Protoc.* **8**, 1494–1512 (2013).
21. F. A. Simão, R. M. Waterhouse, P. Ioannidis, E. V. Kriventseva, E. M. Zdobnov, BUSCO: Assessing genome assembly and annotation completeness with single-copy orthologs. *Bioinformatics* **31**, 3210–3212 (2015).
22. L. Fu, B. Niu, Z. Zhu, S. Wu, W. Li, CD-HIT: Accelerated for clustering the next-generation sequencing data. *Bioinformatics* **28**, 3150–3152 (2012).
23. T. N. Petersen, S. Brunak, G. von Heijne, H. Nielsen, SignalP 4.0: Discriminating signal peptides from transmembrane regions. *Nat. Methods* **8**, 785–786 (2011).
24. S. R. Eddy, A probabilistic model of local sequence alignment that simplifies statistical significance estimation. *PLoS Comput. Biol.* **4**, e1000069 (2008).
25. S. F. Altschul, W. Gish, W. Miller, E. W. Myers, D. J. Lipman, Basic local alignment search tool. *J. Mol. Biol.* **215**, 403–410 (1990).
26. G. F. King, M. C. Gentz, P. Escoubas, G. M. Nicholson, A rational nomenclature for naming peptide toxins from spiders and other venomous animals. *Toxicol.* **52**, 264–276 (2008).
27. F. Hauser, C. J. P. Grimmelikhuijzen, Evolution of the AKH/corazonin/ACP/GnRH receptor superfamily and their ligands in the Protostomia. *Gen. Comp. Endocrinol.* **209**, 35–49 (2014).
28. K. Sunagar *et al.*, Three-fingered RAVERS: Rapid accumulation of variations in exposed residues of snake venom toxins. *Toxins (Basel)* **5**, 2172–2208 (2013).
29. D. G. Tamang, M. H. Saier Jr, The cecropin superfamily of toxic peptides. *J. Mol. Microbiol. Biotechnol.* **11**, 94–103 (2006).
30. S. D. Robinson *et al.*, A comprehensive portrait of the venom of the giant red bull ant, *Myrmecia gulosa*, reveals a hyperdiverse hymenopteran toxin gene family. *Sci. Adv.* **4**, eaau4640 (2018).
31. E. A. Undheim, M. Mobli, G. F. King, Toxin structures as evolutionary tools: Using conserved 3D folds to study the evolution of rapidly evolving peptides. *BioEssays* **38**, 539–548 (2016).
32. P. K. Pallaghy, K. J. Nielsen, D. J. Craik, R. S. Norton, A common structural motif incorporating a cystine knot and a triple-stranded  $\beta$ -sheet in toxic and inhibitory polypeptides. *Protein Sci.* **3**, 1833–1839 (1994).
33. A. A. Walker *et al.*, Buzz kill: Function and proteomic composition of venom from the giant assassin fly *Dolopus genitalis* (Diptera: Asilidae). *Toxins (Basel)* **10**, 456 (2018).
34. A. A. Walker *et al.*, Melt with this kiss: Paralyzing and liquefying venom of the assassin bug *Pristhesancus plagipennis* (Hemiptera: Reduviidae). *Mol. Cell. Proteomics* **16**, 552–566 (2017).
35. K. Furuya *et al.*, Cockroach diuretic hormones: Characterization of a calcitonin-like peptide in insects. *Proc. Natl. Acad. Sci. U.S.A.* **97**, 6469–6474 (2000).
36. B. Shrivastava, A. K. Ghosh, Protein purification, cDNA cloning and characterization of a protease inhibitor from the Indian tasar silkworm, *Antheraea mylitta*. *Insect Biochem. Mol. Biol.* **33**, 1025–1033 (2003).
37. L. Wang, J.-Y. Zhu, C. Qian, Q. Fang, G.-Y. Ye, Venom of the parasitoid wasp *Pteromalus puparum* contains an odorant binding protein. *Arch. Insect Biochem. Physiol.* **88**, 101–110 (2015).
38. H. Dirksen, Insect ion transport peptides are derived from alternatively spliced genes and differentially expressed in the central and peripheral nervous system. *J. Exp. Biol.* **212**, 401–412 (2009).
39. E. A. Undheim *et al.*, Weaponization of a hormone: Convergent recruitment of hyperglycemic hormone into the venom of arthropod predators. *Structure* **23**, 1283–1292 (2015).
40. F. Coste *et al.*, Crystal structure of Diedel, a marker of the immune response of *Drosophila melanogaster*. *PLoS One* **7**, e33416 (2012).
41. T. J. Nelson *et al.*, Calxectin: A signaling protein that binds calcium and GTP, inhibits potassium channels, and enhances membrane excitability. *Proc. Natl. Acad. Sci. U.S.A.* **93**, 13808–13813 (1996).
42. Y.-T. Miao, Y. Deng, H.-K. Jia, Y.-D. Liu, M.-L. Hou, Proteomic analysis of watery saliva secreted by white-backed planthopper, *Sogatella furcifera*. *PLoS One* **13**, e0193831 (2018).
43. G. Delgado-Prudencio, L. D. Possani, B. Becerril, E. Ortiz, The dual  $\alpha$ -amidation system in scorpion venom glands. *Toxins (Basel)* **11**, 425 (2019).
44. N. Jiang *et al.*, PHM is required for normal developmental transitions and for biosynthesis of secretory peptides in *Drosophila*. *Dev. Biol.* **226**, 118–136 (2000).
45. A. A. Walker *et al.*, The assassin bug *Pristhesancus plagipennis* produces two distinct venoms in separate gland lumens. *Nat. Commun.* **9**, 755 (2018).
46. F. Seifert *et al.*, Glutaminyl cyclases display significant catalytic proficiency for glutamyl substrates. *Biochemistry* **48**, 11831–11833 (2009).
47. J. D. Osteen *et al.*, Subtype-selective spider toxins implicate  $\text{Na}_v1.1$  voltage-gated sodium channels in mechanical pain. *Nature* **534**, 494–499 (2016).
48. N. J. Saez, B. Cristofori-Armstrong, R. Anangi, G. F. King, A strategy for production of correctly folded disulfide-rich peptides in the periplasm of *E. coli*. *Methods Mol. Biol.* **1586**, 155–180 (2017).
49. A. Wahedi, G. Gäde, J.-P. Paluzzi, Insight into mosquito GnRH-related neuropeptide receptor specificity revealed through analysis of naturally occurring and synthetic analogs of this neuropeptide family. *Front. Endocrinol. (Lausanne)* **10**, 742 (2019).
50. A. Wahedi, J.-P. Paluzzi, Molecular identification, transcript expression, and functional deorphanization of the adipokinetic hormone/corazonin-related peptide receptor in the disease vector, *Aedes aegypti*. *Sci. Rep.* **8**, 2146 (2018).
51. K. K. Hansen *et al.*, Discovery of a novel insect neuropeptide signaling system closely related to the insect adipokinetic hormone and corazonin hormonal systems. *J. Biol. Chem.* **285**, 10736–10747 (2010).
52. A. Oryan, A. Wahedi, J. V. Paluzzi, Functional characterization and quantitative expression analysis of two GnRH-related peptide receptors in the mosquito, *Aedes aegypti*. *Biochem. Biophys. Res. Commun.* **497**, 550–557 (2018).
53. S. A. Nixon, N. J. Saez, V. Herzig, G. F. King, A. C. Kotze, The antitrypanosomal diarylamidines, diminazene and pentamidine, show anthelmintic activity against *Haemonchus contortus* in vitro. *Vet. Parasitol.* **270**, 40–46 (2019).
54. G. F. King, M. C. Hardy, Spider-venom peptides: Structure, pharmacology, and potential for control of insect pests. *Annu. Rev. Entomol.* **58**, 475–496 (2013).
55. V. Herzig *et al.*, Animal toxins–Nature’s evolutionary-refined toolkit for basic research and drug discovery. *Biochem. Pharmacol.* **181**, 114096 (2020).
56. R. W. Gwadz *et al.*, Effects of magainins and cecropins on the sporogonic development of malaria parasites in mosquitoes. *Infect. Immun.* **57**, 2628–2633 (1989).
57. H. Akuffo, D. Hultmark, A. Engstöm, D. Frohlich, D. Kimbrell, *Drosophila* antibacterial protein, cecropin A, differentially affects non-bacterial organisms such as *Leishmania* in a manner different from other amphipathic peptides. *Int. J. Mol. Med.* **1**, 77–82 (1998).
58. M. C. Rodriguez *et al.*, Effect of a cecropin-like synthetic peptide (Shiva-3) on the sporogonic development of *Plasmodium berghei*. *Exp. Parasitol.* **80**, 596–604 (1995).
59. A. C. Kotze *et al.*, Exploring the anthelmintic properties of Australian native shrubs with respect to their potential role in livestock grazing systems. *Parasitology* **136**, 1065–1080 (2009).
60. V. J. Lynch, Inventing an arsenal: Adaptive evolution and neofunctionalization of snake venom phospholipase A2 genes. *BMC Evol. Biol.* **7**, 2 (2007).
61. F. Kawamoto, N. Kumada, “Biology and venoms of Lepidoptera” in *Handbook of Natural Toxins, Insect Poisons, Allergens and Other Invertebrate Venoms*, A. T. Tu, Ed. (Dekker, New York, 1984), vol. 2, chap. 9, pp. 291–332.
62. D. D. Spadacci-Morena, M. A. M. Soares, R. H. P. Moraes, I. S. Sano-Martins, J. M. Sciani, The urticating apparatus in the caterpillar of *Lonomia obliqua* (Lepidoptera: Saturniidae). *Toxicol.* **119**, 218–224 (2016).
63. F. Kawamoto, C. Suto, N. Kumada, Studies on the venomous spicules and spines of moth caterpillars. I. Fine structure and development of the venomous spicules of the *Euproctis* caterpillars. *Jpn. J. Med. Sci. Biol.* **31**, 291–299 (1978).
64. P. M. Gilmer, A comparative study of the poison apparatus of certain lepidopterous larvae. *Ann. Entomol. Soc. Am.* **18**, 203–239 (1925).
65. A. A. Walker, M. J. Hernández-Vargas, G. Corzo, B. G. Fry, G. F. King, Giant fish-killing water bug reveals ancient and dynamic venom evolution in Heteroptera. *Cell. Mol. Life Sci.* **75**, 3215–3229 (2018).
66. E. A. Undheim *et al.*, Clawing through evolution: Toxin diversification and convergence in the ancient lineage Chilopoda (centipedes). *Mol. Biol. Evol.* **31**, 2124–2148 (2014).
67. D. L. Brinkman *et al.*, Transcriptome and venom proteome of the box jellyfish *Chironex fleckeri*. *BMC Genomics* **16**, 407 (2015).
68. N. Peiren *et al.*, The protein composition of honeybee venom reconsidered by a proteomic approach. *Biochim. Biophys. Acta* **1752**, 1–5 (2005).
69. M. Y. Sachkova *et al.*, Toxin-like neuropeptides in the sea anemone *Nematostella* unravel recruitment from the nervous system to venom. *Proc. Natl. Acad. Sci. U.S.A.* **117**, 27481–27492 (2020).
70. R. Arvidson *et al.*, Parasitoid jewel wasp mounts multipronged neurochemical attack to hijack a host brain. *Mol. Cell. Proteomics* **18**, 99–114 (2019).
71. S. D. Robinson *et al.*, Hormone-like peptides in the venoms of marine cone snails. *Gen. Comp. Endocrinol.* **244**, 11–18 (2017).
72. S. Zhu *et al.*, Experimental conversion of a defensin into a neurotoxin: Implications for origin of toxic function. *Mol. Biol. Evol.* **31**, 546–559 (2014).
73. C.-W. Vogel *et al.*, “Structure and function of cobra venom factor, the complement-activating protein in cobra venom” in *Natural Toxins 2: Structure, Mechanism of Action, and Detection*, B. R. Singh, A. T. Tu, Eds. (Springer US, Boston, MA, 1996), pp. 97–114.
74. S. H. Drukewitz, L. Bokelmann, E. A. B. Undheim, B. M. von Reumont, Toxins from scratch? Diverse, multimodal gene origins in the predatory robber fly *Dasygogon diadema* indicate a dynamic venom evolution in dipteran insects. *Gigascience* **8**, giz081 (2019).
75. E. O. Martinson, Mrinalini, Y. D. Kelkar, C. H. Chang, J. H. Werren, The evolution of venom by co-option of single-copy genes. *Curr. Biol.* **27**, 2007–2013.e8 (2017).
76. M. E. Epstein, J. F. Corrales, Twenty-five new species of Costa Rican Limacodidae (Lepidoptera: Zygaenoidea). *Zootaxa* **701**, 1–86 (2004).
77. S. A. Nixon *et al.*, Where are all the anthelmintics? Challenges and opportunities on the path to new anthelmintics. *Int. J. Parasitol. Drugs Drug Resist.* **14**, 8–16 (2020).
78. S. Suwansa-Ard *et al.*, Gonadotropin-releasing hormone and adipokinetic hormone/corazonin-related peptide in the female prawn. *Gen. Comp. Endocrinol.* **236**, 70–82 (2016).
79. D. Hultmark, H. Steiner, T. Rasmuson, H. G. Boman, Insect immunity. Purification and properties of three inducible bactericidal proteins from hemolymph of immunized pupae of *Hyalophora cecropia*. *Eur. J. Biochem.* **106**, 7–16 (1980).
80. G. Corzo, S. Adachi-Akahane, T. Nagao, Y. Kusui, T. Nakajima, Novel peptides from assassin bugs (Hemiptera: Reduviidae): Isolation, characterization and biological characterization. *FEBS Lett.* **499**, 256–261 (2001).
81. F. C. Cardoso *et al.*, Identification and characterization of ProTx-III [ $\mu$ -TRTX-Tp1a], a new voltage-gated sodium channel inhibitor from venom of the tarantula *Thrixopelma pruriens*. *Mol. Pharmacol.* **88**, 291–303 (2015).